Measurement of the spatial backscattering impulse-response at short length scales with polarized enhanced backscattering

Andrew J. Radosevich,[1,*] Nikhil N. Mutyal,[1] Vladimir Turzhitsky,[1] Jeremy D. Rogers,[1] Ji Yi,[1] Allen Taflove,[2] and Vadim Backman[1]

[1]*Biomedical Engineering, Northwestern University, Evanston, Illinois 60208, USA*

[2]*Electrical Engineering and Computer Science, Northwestern University, Evanston, Illinois 60208, USA*

**Corresponding author: arad@u.northwestern.edu*

Received August 9, 2011; revised October 25, 2011; accepted November 2, 2011; posted November 4, 2011 (Doc. ID 152621); published December 13, 2011

In this Letter, we describe an easy to implement technique to measure the spatial backscattering impulse-response at length scales shorter than a transport mean free path with resolution of better than 10 μm using the enhanced backscattering phenomenon. This technique enables spectroscopic measurements throughout the visible range and sensitivity to all polarization channels. Through a combination of Monte Carlo simulations and experimental measurements of latex microspheres, we explore the various sensitivities of our technique to both intrinsic sample properties and extrinsic instrumental properties. We conclude by demonstrating the extraordinary sensitivity of our technique to the shape of the scattering phase function, including higher order shape parameters than the anisotropy factor (or first moment).

OCIS codes: 030.1670, 290.1350, 290.4210.

The spatial backscattering impulse-response at length scales shorter than a transport mean free path l_s^* is highly sensitive to the shape of the scattering phase function due to the fact that rays exiting within this regime have undergone relatively few scattering events. Typically this measurement is accomplished using a lens to focus the illumination beam to a near impulse on the sample surface. A CCD camera then detects the spatial distribution of backscattered light at the sample surface. With this design, the full azimuthal backscattering distribution can easily be measured for each polarization channel [1]. Still, a true impulse can never be achieved and information at short length scales is lost to an optical mask (~mm diameter) needed to reject specular reflections. Thus in media such as biological tissue with long l_s^* on the order of 1 mm, information about the shape of the phase function is extremely difficult to measure experimentally. As an alternative to overcome these difficulties, here we report a simple bench-top instrument using polarized enhanced backscattering (EBS) to first measure the backscattering distribution in the angular domain and subsequently convert to the spatial domain through inverse Fourier transformation.

EBS is an angular intensity peak centered in the exact backscattering direction that is formed by the summed diffraction pattern from all sets of time-reversed path-pairs within a scattering medium (a direct consequence of the reciprocity theorem) [2]. Conceptually, it is useful to think of each time-reversed path pair as a single Young's double pinhole experiment. For a single time-reversed path pair with rays exiting at a particular spatial separation, the diffraction pattern is the Fourier transform of two delta functions (cosine pattern). For a semi-infinite medium under plane wave illumination the distribution of spatial separations for all time-reversed path-pairs is given by the spatial backscattering impulse-response for multiply scattered light in the exact backward direction $p(x, y)$. As a result, in an idealized case the EBS peak $I_{\mathrm{EBS}}(\theta_x, \theta_y)$ is simply the Fourier transform of $p(x, y)$. However, as we will demonstrate, the dependencies are more complex:

$$I_{\mathrm{EBS}}(\theta_x, \theta_y) = \mathcal{F}\{p(x, y) \cdot pc(x, y) \cdot s(x, y) \cdot c(x, y) \cdot \mathrm{mtf}(x, y)\}, \quad (1)$$

where $\mathcal{F}$ denotes the Fourier transform operation, pc specifies the degree of phase correlation between the forward and reverse path, s represents the effective distribution of rays that remain within the illumination spot, c is the spatial coherence function, and mtf is the modulation transfer function of the optical instrument. Within the $\mathcal{F}$ operation, p and pc represent instrinsic sample properties while s, c, and mtf represent extrinsic instrument properties. Each of these functions will be described in further detail in the following paragraphs.

The experimentally measurable p_{eff} is found by computing the inverse Fourier transform of the EBS peak:

$$p_{\mathrm{eff}} = \mathcal{F}^{-1}\{I_{\mathrm{EBS}}(\theta_x, \theta_y)\}. \quad (2)$$

For sample characterization, the functions p and pc are of prime interest. In principle these intrinsic parameters can be found by dividing p_{eff} by functions s, c, and mtf. However, in practice this will amplify noise and a reliable result can be difficult to obtain. Alternatively, a more stable approach that we follow in this Letter is to convert theory into the experimentally observable p_{eff} before comparison with experiment.

Our experimental instrument is shown in Fig. 1. An illumination source (xenon lamp with finite spatial coherence length L_{sc} or broadband laser with $L_{sc} = \infty$) is collimated by lens L_1 and polarized by linear polarizer P before being directed onto the scattering sample via a nonpolarizing 50/50 beam splitter B. Backscattered light is then collected by B and passes through a linear analyzer A before being focused onto a CCD camera with a lens L_2. A liquid crystal tunable filter attached to the

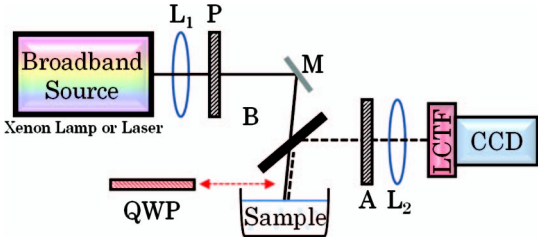

Fig. 1. EBS instrument. Collimating lens L_1 ($f = 200$ mm), linear polarizer P, mirror M, beam splitter B, quarter wave plate QWP, linear analyzer A, Fourier lens L_2 ($f = 100$ mm), liquid crystal tunable filter LCTF.

CCD separates the backscattered light into its component wavelengths. All polarization combinations are achieved by rotating P and/or inserting a quarter wave plate (QWP) between B and the sample.

Information regarding the processing of experimental and Monte Carlo simulated EBS data can be found in detail in other publications [3,4]. It should be noted that all experimental data is scaled by a constant multiplicative factor of 0.65 to obtain a full match with Monte Carlo simulation [4]. This type of one parameter fit is common in EBS literature [5]. In this Letter, all experiments and Monte Carlo simulations are for aqueous latex microsphere suspensions (10% solids by weight) that are diluted in deionized water to achieve different values of l_s^*. After retrieving the experimental EBS peak, the spatial distribution of backscattered light is computed using Eq. (2). According to the properties of the discrete Fourier transform, the spatial resolution Δs is related to the angular resolution $\Delta\theta$ by

$$\Delta s = \frac{\lambda}{n \cdot \Delta\theta}, \tag{3}$$

where λ is the illumination wavelength and n is the number of pixels in the x or y direction. Our instrument collects angles up to 7.5776° with 0.0074° resolution. Within the visible range of illumination this corresponds to a spatial extent of >1500 μm with <10 μm resolution.

Strictly speaking the reciprocity theorem is only fully valid for polarization preserving channels (i.e., linear copolarized xx or helicity preserving $++$) [2]. For these channels, each ray has a time-reversed partner that exits with the same accumulated phase and $pc = 1$ for all x, y positions. However, in the orthogonal polarization channels (i.e., linear cross-polarized xy or opposite helicity $+-$) not all scattering rotations are reversible. As a result, the forward and reverse paths may exit with different phases and pc does not necessarily equal 1. Following the calculations of [6], pc in the orthogonal channels can be approximated from the degree of linear ($\mathrm{dlp} = \frac{(xx)-(xy)}{(xx)+(xy)}$) and circular ($\mathrm{dcp} = \frac{(++)-(+-)}{(++)+(+-)}$) polarization:

$$pc_{xy}(r) = \frac{\mathrm{dlp}(r) + \mathrm{dcp}(r)}{1 - \mathrm{dlp}(r)} pc_{+-}(r) = \frac{2 \cdot \mathrm{dlp}(r)}{1 - \mathrm{dcp}(r)}. \tag{4}$$

Figure 2(a) shows function pc for the four measured polarization channels. For very short length scales, rays undergo relatively few scattering events and pc is nearly 1. As the exit radius increases, the average number of scattering events also increases. As a result, a greater

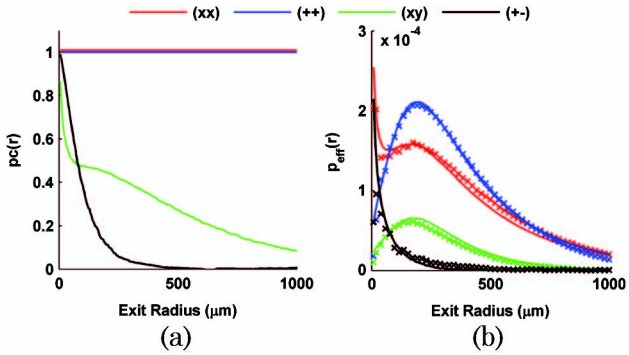

Fig. 2. Polarization sensitivities. (a) Function pc for the four measured polarization channels as a function of exit radius. (b) Experimental (symbols) and simulation (lines) p_{eff}. Sample: 0.65 μm diameter sphere with $l_s^* = 205$ μm at 633 nm. Spot size = 6000 μm and $L_{\mathrm{sc}} = \infty$. Simulation scaled by 0.65 to obtain match with experiment.

proportion of rays travel through irreversible paths and $pc \to 0$ as $r \to \infty$ [2]. Figure 2(b) shows the excellent agreement between experiment and simulation for p_{eff} measured from each of the four polarization channels.

Since realistic experiments have finite illumination beam extent, an effective distribution of rays that remains within the illumination spot (and therefore possess a time-reversed partner) must be found. This can be obtained by computing the normalized autocorrelation function (ACF) of the illumination pattern A incident on the scattering sample [4]:

$$s(x, y) = \mathrm{ACF}\{A(x, y)\}. \tag{5}$$

In our case, a circular beam is used and A is a top hat function (i.e., $A = 1$ within the illumination spot and 0 otherwise). For each spot size, s begins at 1 and decreases to 0 when the path-pair separation is larger than the beam diameter. Figure 3(a) shows function s for two illumination spot sizes. Figure 3(b) shows excellent agreement between the experiment and simulation p_{eff} for 2000 and 7000 μm spot sizes.

Another consideration for the measurement of p_{eff} is function c, which describes the ability for path-pairs to interfere when using a partial spatial coherence source.

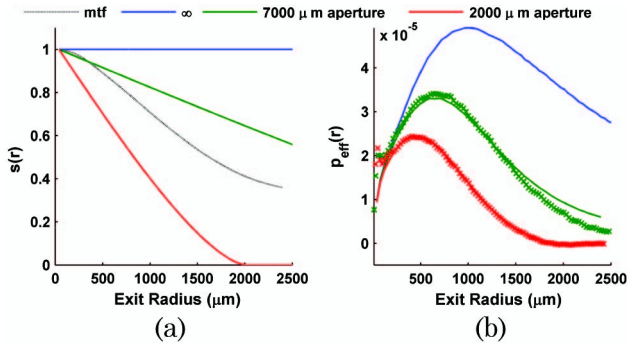

Fig. 3. Illumination beam spot size sensitivities. (a) s as a function of exit radius for two beam spot sizes. (b) Comparison between experiment (symbols) and simulation (lines) for the different beam spot sizes using $++$ polarization. Sample: 0.65 μm diameter sphere with $l_s^* = 950$ μm at 633 nm. $L_{\mathrm{sc}} = \infty$. Simulation scaled by 0.65.

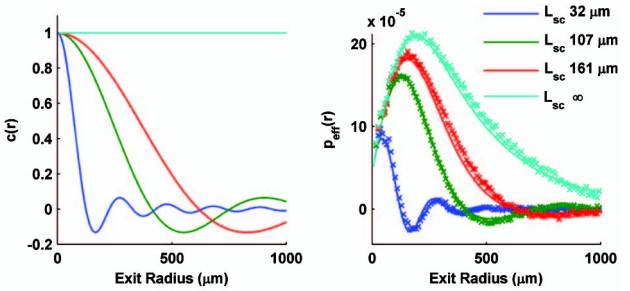

Fig. 4. Sensitivities to the spatial coherence of the illumination. (a) Function c for different L_{sc}. (b) Comparison between experiment (symbols) and simulation (lines) for different L_{sc} using $++$ polarization. Sample: 0.65 μm diameter sphere with $l_s^* = 205$ μm at 633 nm. Spot size = 6000 μm and $L_{sc} = \infty$. Simulation scaled by 0.65.

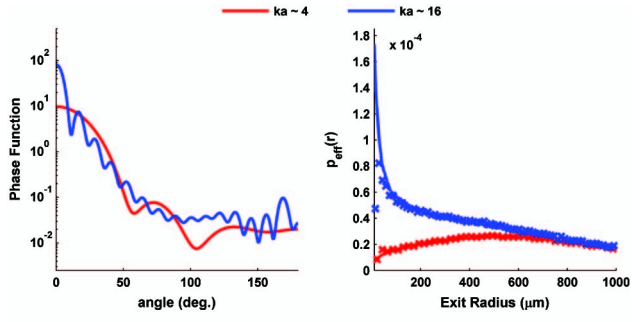

Fig. 5. Sensitivity of EBS to the phase function. (a) Phase function for two microsphere samples with the same g but different ka. (b) Corresponding p_{eff} for $++$ polarization shows a large difference in shape at short length-scales. $ka \sim 4$: 0.65 μm diameter sphere at 633 nm. $ka \sim 16$: 2.1 μm diameter sphere at 558 nm. Spot size = 2000 μm and $L_{sc} = \infty$. Simulation scaled by 0.65.

For a typical laser source, L_{sc} is sufficiently large that over the extent of the beam spot size it can be considered spatially coherent (i.e., $c = 1$). However, even for illumination with very short L_{sc} (e.g., sunlight or xenon source) an EBS peak is formed. In this case, function c can be found according to the van-Cittert Zernike theorem. For our instrument, function c takes the form of a first-order Bessel function of the first kind J_1 [3]:

$$c(r) = \frac{2J_1(r/L_{sc})}{r/L_{sc}}. \tag{6}$$

Figure 4(a) shows function c for illumination with four different L_{sc} possible with our instrument. Figure 4(b) shows the agreement between the experiment and simulation p_{eff} for each of these L_{sc}.

For any imaging system the mtf describes the ability to capture information from different spatial frequencies. As such, the measurement of p_{eff} will also be modulated by the mtf. To determine our system's mtf [shown in Fig. 3(a)] we computed the Fourier transform of the point spread function measured by placing a mirror in the sample plane and imaging the laser onto the CCD.

As a final demonstration of the sensitivity of our technique to fine details in the scattering phase function, we measure two suspensions of microspheres with the same l_s^* (1000 μm) and anisotropy factor g (0.87) but different size parameter ka (where k is the wavenumber in water and a is the microsphere radius). Figure 5(a) displays the two samples' phase functions. Although they are generally similar in shape, the sample with higher ka has many higher frequency oscillations in accordance with Mie theory. In Fig. 5(b) we demonstrate that these higher frequency oscillations have a profound effect on the shape of p_{eff} at short length scales. These slight differences are readily distinguishable using the technique presented in this Letter.

In summary we have presented EBS as a useful method to measure the backscattering impulse-response at small length-scales where information about the phase function is preserved. We first discussed the various sample dependent and experimental variables that affect the measurement and then provided a demonstration of its extraordinary sensitivity to the shape of the phase function.

This study was supported by National Institutes of Health (NIH) grant numbers RO1CA128641 and R01EB003682. A. J. Radosevich is supported by a National Science Foundation (NSF) Graduate Research Fellowship under Grant No. DGE-0824162.

References

1. A. Hielscher, A. Eick, J. Mourant, D. Shen, J. Freyer, and I. Bigio, Opt. Express **1**, 441 (1997).
2. R. Lenke and G. Maret, in *Scattering in Polymeric and Colloidal Systems* (2000).
3. V. Turzhitsky, J. D. Rogers, N. N. Mutyal, H. K. Roy, and V. Backman, IEEE J. Sel. Top. Quantum Electron. **16**, 619 (2010).
4. A. J. Radosevich, J. D. Rogers, V. Turzhitsky, N. N. Mutyal, J. Yi, H. K. Roy, and V. Backman, "Polarized enhanced backscattering spectroscopy for characterization of biological tissues at subdiffusion length scales," IEEE J. Sel. Top. Quantum Elect., to be published.
5. M. Ospeck and S. Fraden, Phys. Rev. E **49**, 4578 (1994).
6. R. Lenke and G. Maret, Eur. Phys. J. B **17**, 171 (2000).